# A 4-Yr Climatology of Cold-Season Bow Echoes over the Continental United States

PATRICK C. BURKE* AND DAVID M. SCHULTZ

*Cooperative Institute for Mesoscale Meteorological Studies, University of Oklahoma, and NOAA/National Severe Storms Laboratory, Norman, Oklahoma*

(Manuscript received 15 April 2003, in final form 27 April 2004)

ABSTRACT

A search of radar mosaics and level-II Weather Surveillance Radar-1988 Doppler (WSR-88D) data revealed 51 cold-season (October–April) bow echoes that occurred in the contiguous United States from 1997–98 to 2000–01. Proximity soundings indicated mean 0–2.5-, 0–5-, and 5–10-km shear values of 14, 23, and 19 m $s^{-1}$, respectively. Mean CAPE was 1366 J $kg^{-1}$. Most bow echoes developed from squall lines, groups of cells, or squall lines overtaking cells that originated in the path of the squall line. Overall, cell mergers occurred just prior to the development of 34 (67%) of the 51 bow echoes, and embedded supercells were present in the mature stage of 22 (43%) bow echoes.

Nine severe, long-lived bow echoes (LBEs) were identified, and seven of these had damage paths that met derecho criteria. LBEs developed in strongly forced, dynamic synoptic patterns with low to moderate instability. As in previous observational studies, proximity soundings suggested that LBEs are possible within much wider ranges of sampled CAPE and shear than idealized numerical modeling studies have indicated.

Cold-season bow echoes formed overwhelmingly (47 of 51) in southwesterly 500-mb flow. Twenty (39%) bow echoes formed in a Gulf coast synoptic pattern that produced strong shear and moderate instability over the southeastern United States. Nineteen (37%) and seven (14%) bow echoes, respectively, formed in the plains and east synoptic patterns, which resemble classic severe weather outbreak patterns. Four (8%) bow echoes developed in a northwest flow synoptic pattern that produced strong shear and moderate instability over the southern plains.

## 1. Introduction

The bow echo (Fujita 1978) is a distinctive convective structure named for its bow- or arc-shaped appearance on plan-view radar reflectivity displays. Bow echoes are frequently associated with widespread damaging winds at the surface. Johns and Hirt (1987) showed that downbursts from long-lived intense bow echoes called derechos (Hinrichs 1888) account for the majority of casualties and damage resulting from convectively induced nontornadic winds in the United States.

Many observational and numerical studies of bow echoes and derechos have been performed (see the reviews in Przybylinski 1995; Weisman 2001; Wakimoto 2001). Although several climatological studies have investigated bow echoes and derechos (Table 1), relatively few cold-season bow echoes have been documented, and no study has discussed nonderecho-producing cold-season bow echoes.

The purpose of this paper is to investigate cold-season bow echoes (cold season is defined as 1 October–30 April), inclusive of nonderecho-producing bow echoes. Data and methodology are discussed in section 2. Section 3 documents 51 bow echoes, their severity, and their environments over four cold seasons. Synoptic patterns associated with cold-season bow echoes are examined in section 4. Conclusions are presented in section 5.

## 2. Data and methodology

All severe thunderstorm wind reports were obtained for the four cold seasons (October–April) from 1997–98 to 2000–01 using the National Oceanic and Atmospheric Administration (NOAA) publication *Storm Data*. For the same period, an archive of hourly national radar mosaics, comprising Weather Surveillance Radar-1988 Doppler (WSR-88D) data at 4-km horizontal resolution available online at the National Climatic Data Center (NCDC) Web site (http://www4.ncdc.noaa.gov/cgi-win/wwcgi.dll?WWNEXRAD~Images2; Williams and Loehrer 1996), was examined for bow-shaped echoes. There were no objective criteria for identifying bow echoes, but all curved radar echoes of any scale that appeared to be associated with deep moist convection

* Current affiliation: NOAA/National Weather Service, Goodland, Kansas.

*Corresponding author address:* Patrick C. Burke, National Weather Service, 920 Armory Rd., Goodland, KS 67735-9273.
E-mail: patrick.burke@noaa.gov

TABLE 1. Climatological investigations of bow echoes and derechos.

| Article | Subject | Seasons | No. of events | No. of cold-season events |
|---|---|---|---|---|
| Johns and Hirt (1987) | Derechos (1980–93) | All | 70 | 0 |
| Johns et al. (1990) | Strongest derechos (1983–87) | Warm season | 14 | 0 |
| Bentley and Mote (1998) | Derechos* (1986–95) | All | 112 | 36 |
| Bentley and Mote (2000) | Derechos* (1986–95) | Cold season | 14 | 14 |
| Klimowski et al. (2000) | Bow echoes (1996–2000) | Not given | 110 | Not given |
| Evans and Doswell (2001) | Derechos (1983–93) | All (1988–93) and warm season (1983–87) | 67 | 12 |
| Bentley and Sparks (2003) | Derechos* (1996–2000) | All | 118 | 33 |
| This study (2003) | Bow echoes (1997–2001) | Cold season | 51 | 51 |

* Bentley and Mote (1998), Bentley and Mote (2000), and Bentley and Sparks (2003) used a slightly modified form of the derecho criteria, which Johns and Hirt (1987) defined.

were included as possible bow echoes. There were only 20 days for which radar mosaics were entirely unavailable. For completeness, each severe thunderstorm wind report from those days was examined for the existence of a possible bow echo. These procedures produced a list of 150 possible bow echoes, 144 of which occurred at or near the time and location of at least one severe thunderstorm wind report.

The temporal resolution of the national radar mosaics was usually 1 h, with images posted for the top of each hour. Some mosaics were missing, and others represented times of 15, 30, or 45 min after the hour. For the period studied, excluding the 20 days for which radar mosaics were entirely unavailable, the maximum gap between mosaics was 1 h and 45 min. Therefore, any bowing radar echo that persisted for at least 105 min should have appeared on at least one mosaic. The spatial resolution of the mosaics is somewhat coarse, but it is sufficient to identify most bow echoes, excluding only those of small horizontal extent.

### *a. Defining a bow echo*

Precise and consistent criteria for what constitutes a bow echo are rare in the previous literature. Instead, a series of studies has incrementally added to the known radar characteristics, space scales, and time scales associated with bow echoes (see the reviews in Przybylinski 1995; Weisman 2001).

Most bow echoes vary between 20 and 120 km in length (e.g., Fujita 1978; Przybylinski 1995). Przybylinski (1995), however, pointed out that, ''Studies by Wakimoto (1983) and Przybylinski (1988) have shown that in cool-season strong-dynamic environments, small-scale bow echoes of less than 20 km in length and embedded in a larger squall line can be significant severe wind and tornado producers.'' Some bow echoes have been observed to last more than a day (Lee et al. 1992), whereas other bow echoes last only a few hours. When, then, does a crescent-shaped radar echo take on a distinctive identity as a bow echo?

Fujita (1978) described the life cycle of a bow echo as ''a gradual transition from a large, strong, and tall echo to a bow [echo] which often turns into a 'comma-shaped echo.''' Another defining characteristic of bow echoes has traditionally been their direct association with downburst winds (e.g., Fujita and Caracena 1977; Fujita 1978). Klimowski et al. (2000) argue that, ''As downbursts cannot be verified for all bowing structures observed on radar, a somewhat broader definition must be adopted: . . . a bow or crescent-shaped radar echo with a tight reflectivity gradient on the convex (leading) edge, the evolution and horizontal structure of which is consistent with outflow-dominated systems. That is, the bowing echo should demonstrate an increasing radius with time, be associated with very strong winds, and/or exhibit a persistent arc which deviates significantly (in direction or magnitude) from the mean tropospheric wind.''

Presumably, Klimowski et al. (2000) use the term outflow dominated to describe an expanding cold pool, one that spreads beneath and advances beyond the leading edge of the original convective line. An expanding cold pool often controls the evolution of leading-line convection in bow echoes (e.g., Rotunno et al. 1988; Weisman et al. 1988; Weisman 1993; Skamarock et al. 1994); hence, some indication of an expanding cold pool or outflow dominance is appropriate when defining bow echoes. In their definition, Klimowski et al. (2000) indicate some ways that radar data can be used to assess outflow dominance. The best method is to examine the flow character of squall lines and bow echoes using vertical cross sections of storm-relative radial velocity. The necessary data may not be sampled, though, when the convection is far from the radar or moving perpendicular to the radial viewing angle of the radar.

The definition of bow echo given by Klimowski et al. (2000) will serve as the basis for the definition of bow echo for this study. Additionally, a bow echo must have been large enough to appear as a crescent-shaped echo in reflectivity data of 4-km horizontal resolution. No limits were placed on the curvature of bow echoes. The minimum frequency of the NCDC national radar mosaics, at 105 min, sets a necessary lower boundary for the longevity of a bow echo that could be observed in this study. Bow echoes that persisted for less than

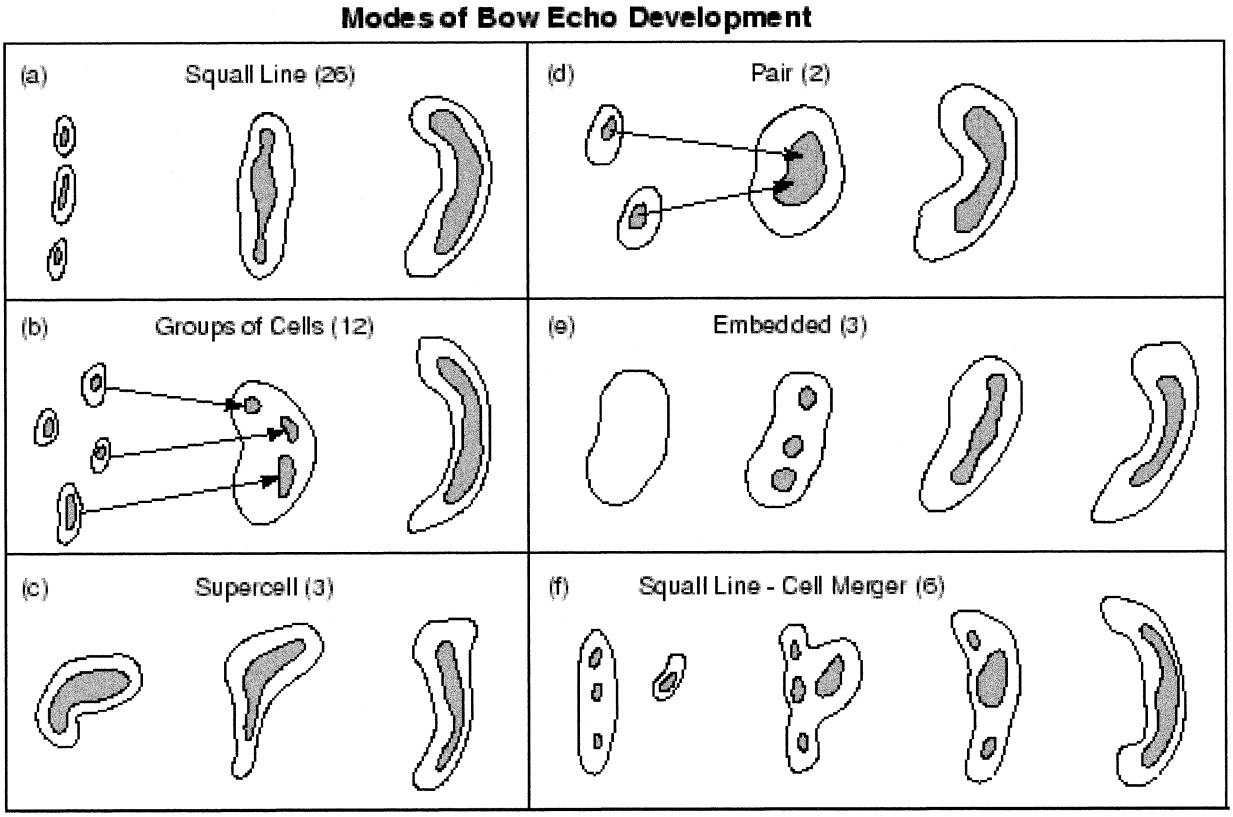


FIG. 1. Convective modes from which bow echoes developed. The number of cold-season bow echoes that developed from each mode for the study period is indicated in parentheses. Shaded areas represent high radar reflectivity values.

105 min may have occurred entirely between the times of two national radar mosaics, rendering them undetectable in this study. Therefore, this climatology may not include every bow echo that occurred, but the 105 min longevity requirement likely excludes only small, short-lived bow echoes.

### *b. Analyzing WSR-88D level-II data*

WSR-88D (Crum and Alberty 1993) level-II data (Crum et al. 1993) were available and used to confirm or deny the existence of a bow echo in 148 of the 150 cases of possible bow echoes. Applying the definition of a bow echo from the previous section to those cases with WSR-88D level-II data yielded 51 bow echoes. The majority of the 150 possible bow echoes had the appearance of a bow echo in the coarse, 4-km WSR-88D reflectivity data, but were determined (based on previous definitions) not to be bow echoes. [In most cases, these events were slightly curved squall lines that did not display an evolution consistent with the definition of bow echoes stated in section 2a. For examples of how this scheme was applied to possible bow echoes, see Burke (2002).]

### *c. Classifying initial convective modes of bow echoes*

Once a bow echo was confirmed using level-II WSR-88D data the initial convective mode from which the bow echo developed was then classified as one of six modes: squall line, group (or cluster), supercell, pair, embedded, and squall-line–cell merger. Klimowski et al. (2000) identified the squall line, group, and supercell modes (Figs. 1a–c) as the three primary initial modes of convection from which their 110 bow echoes developed. Bluestein and Parker (1993) describe the pair (Fig. 1d) as an initial mode for isolated, severe convective storm formation along the dryline in the southern plains states. Bluestein and Jain (1985) also showed that severe squall lines occasionally develop from an embedded mode in which the squall line is embedded in a larger area of weaker, stratiform precipitation (Fig. 1e). The sixth mode for the early development of bow echoes, squall-line–cell merger, can be described as a squall line overtaking either an isolated cell or a group of cells external to the squall line (Fig. 1f). This is distinct from the squall-line mode in which mergers are only between cell members of the original squall line.

*First-echo time* was defined as the time of the first appearance of a 40-dB*Z* echo within the squall line, group of cells, pair of cells, or single cell that eventually

formed a bow echo. First-echo time was unambiguous from level-II WSR-88D data. In some cases, however, level-II WSR-88D data were not available from radars that were near the location of the first echo, and the NCDC national radar mosaics were used to estimate first-echo time to within 30–60 min. *Bow-echo start time* was defined as the time of the first appearance of a bow echo in level-II WSR-88D data at the lowest elevation angle. *Bow-echo end time* was defined as the earliest time when a bow echo (defined by the criteria in this study and lasting for at least 105 min) was no longer identifiable in level-II WSR-88D data at the lowest elevation angle. Bow-echo end time was indeterminable for two bow echoes that proceeded into the Atlantic Ocean, out of range of the WSR-88D network. *Longevity* is defined as the lifetime of the bow echo from bow-echo start time to bow-echo end time.

### *d. Supercells*

Miller and Johns (2000) showed cases in which extreme wind damage was associated with supercells embedded within derechos. This study sought to determine the frequency of supercells in cold-season bow echoes.

*The Glossary of Meteorology* (Glickman 2000) defined a supercell as ''a single, quasi-steady rotating updraft, which persists for a period of time much longer than it takes an air parcel to rise from the base of the updraft to its summit (often much longer than 10–20 minutes).'' Based on this definition, a cell was considered a supercell if the Doppler radar velocity signature of a deep (at least half the depth of the parent cloud as measured by radar), rotating updraft could be followed for 1 h or more. All of the supercells observed during this study persisted for well over 1 h.

### *e. Environmental parameters*

Some of the difficulties in choosing appropriate proximity soundings for deep moist convection have been discussed previously (e.g., Brooks et al. 1994). In this study, proximity soundings were required to have been taken within 300 min (5 h) and 300 km of the path of the bow-echo apex as it appeared in WSR-88D data. Furthermore, the soundings must have been uncontaminated by convection. In some cases, surface temperature and dewpoint varied greatly between the site of the proximity sounding and the eventual path of the bow-echo apex. This occurred primarily when the proximity sounding site was located outside of a moist tongue or on the cool side of a boundary. To better represent the thermodynamic environment in which bow echoes formed, the surface observations in some soundings were substituted with surface observations taken immediately ahead of the convection at bow-echo start time.

Shear was defined as the vector difference between winds at the top of a layer and the bottom of a layer. The 0–2.5-, 0–5-, and 5–10-km above ground level (AGL) shear vectors were computed to investigate low-level, midlevel, and upper-level shear, respectively. Convective available potential energy (CAPE) and the mean mixing ratio in the lowest 100 hPa AGL were computed to measure instability and low-level moisture, respectively. Lifting condensation level (LCL), level of free convection (LFC), and CAPE were calculated using the most unstable parcels in the proximity soundings.

## 3. Results

During the four cold seasons (October–April) from 1997–98 to 2000–01, 51 bow echoes were identified (Table 2). Bow echoes were observed in 22 states, primarily south of 45°N and east of the Rocky Mountains (Fig. 2). At least one bow echo was observed in each calendar month (Fig. 3), with the majority (84%) of bow echoes occurring in February (15), March (10), and April (18). Bow echoes primarily occurred in the southeast United States between January and March, and in the plains from late February through April.

### *a. Initial convective modes of bow echoes*

The most common convective modes from which bow echoes developed were squall line (26), group (12), and squall-line–cell merger (6) (Fig. 1). There did not appear to be any preferred geographical regions in which bow echoes developed from particular modes. Cell mergers occurred just prior to the formation of 34 (67%) of the 51 bow echoes. This agrees well with Klimowski et al. (2000) who reported that ''the majority (70%) of bow echoes observed to evolve from isolated cells or groups of storms occurred immediately after some type of convective merger.'' Cell mergers were noted with 11 (91%) of the 12 bow echoes that evolved from the group mode. However, cell mergers were observed in only 5 (19%) of 26 bow echoes that evolved from squall lines, excluding those of the squall-line–cell merger mode. In contrast, Klimowski et al. (2000) reported cell mergers in 50% of squall-line bow echoes in their dataset.

Environmental variables were compared among the two modes for which more than 10 proximity soundings were obtained: squall line (21) and group (13). Bow echoes that developed from the group mode generally had both higher LCL heights and higher LFC heights. The mean LCL height was 1227 m for the group mode, compared to 727 m for the squall-line mode. The mean LFC height was 1833 m for the group mode and 1422 m for the squall-line mode. The other environmental variables studies did not differ greatly between the two modes.

For all bow echoes, the majority of first-echo times occurred in the afternoon with a strong spike between 1800 and 1900 UTC (Fig. 4a). First-echo times were observed much less frequently in the overnight or early morning hours. A maximum in the distribution of bow-

TABLE 2. Bow echoes and their attributes.

| Date | Radar | Development mode | Severe thunderstorm wind reports | Tornado reports | Synoptic pattern |
|---|---|---|---|---|---|
| 1997 | | | | | |
| 7 Oct | Amarillo, TX | Squall line | 0 | 0 | Plains |
| 1998 | | | | | |
| 5 Jan | Shreveport, LA | Pair | 6 | 0 | Plains |
| 21 Jan | Lake Charles, LA | Squall line | 10 | 0 | Gulf |
| 22 Jan | Mobile, AL | Squall line | 5 | 0 | Gulf |
| 10 Feb | Houston, TX | Squall line | 130 (LBE) | 8 | Gulf |
| 17 Feb | Tallahassee, FL | Squall line | 3 | 0 | Gulf |
| 21 Feb | Austin, TX | Squall line | 1 | 0 | Gulf |
| 21 Feb | Austin, TX | Squall line | 1 | 0 | Gulf |
| 22 Feb | Mobile, AL | Embedded | 20 | 2 | Gulf |
| 26 Feb | Lake Charles, LA | Cluster | 52 (LBE) | 3 | Gulf |
| 8 Mar | Jacksonville, FL | Squall line | 7 | 0 | Gulf |
| 20 Mar | Miami, FL | Cluster | 1 | 0 | Gulf |
| 26 Mar | Goodland, KS | Cluster | 1 | 0 | Plains |
| 6 Apr | Wichita, KS | Squall line | 3 | 0 | Plains |
| 6 Apr | Tulsa, OK | Squall line | 16 | 0 | Plains |
| 19 Apr | Tallahassee, FL | Squall-line/cell merger | 4 | 1 | Gulf |
| 4 Oct | Kansas City, MO | Cluster | 1 | 0 | Plains |
| 1999 | | | | | |
| 17 Jan | Nashville, TN | Cluster | 83 (LBE) | 12 | East |
| 17 Feb | Houston, TX | Embedded | 0 | 0 | Gulf |
| 5 Mar | Memphis, TN | Squall-line/cell merger | 2 | 0 | East |
| 2 Apr | Norman, OK | Squall line | 6 | 0 | Plains |
| 2 Apr | Wichita, KS | Squall line | 12 | 0 | Plains |
| 25 Apr | Little Rock, AR | Cluster | 11 | 0 | Plains |
| 26 Apr | San Angelo, TX | Squall line | 1 | 0 | Plains |
| 26 Apr | San Angelo, TX | Squall line | 75 (LBE) | 6 | Plains |
| 3 Dec | Wichita, KS | Squall-line/cell merger | 12 | 0 | Plains |
| 2000 | | | | | |
| 7 Feb | Houston, TX | Supercell | 0 | 0 | NW flow |
| 14 Feb | Knoxville, TN | Squall line | 17 | 0 | Gulf |
| 14 Feb | Pocatello, ID | Squall line | 8 | 6 | Mountain |
| 18 Feb | Charleston, WV | Squall line | 0 | 0 | East |
| 22 Feb | Norman, OK | Squall line | 3 | 0 | Plains |
| 24 Feb | Lubbock, TX | Squall line | 3 | 1 | Plains |
| 29 Feb | Davenport, IA | Pair | 0 | 0 | East |
| 11 Mar | Atlanta, GA | Cluster | 6 | 0 | Gulf |
| 16 Mar | Tallahassee, FL | Cluster | 7 | 0 | Gulf |
| 27 Mar | Shreveport, LA | Cluster | 20 | 0 | NW flow |
| 12 Apr | Austin, TX | Squall-line/cell merger | 3 | 0 | Gulf |
| 12 Apr | Lake Charles, LA | Squall line | 4 | 0 | Gulf |
| 17 Apr | Charleston, WV | Squall line | 0 | 0 | East |
| 24 Apr | Lake Charles, LA | Squall-line/cell merger | 4 | 0 | Gulf |
| 24 Apr | Amarillo, TX | Supercell | 2 | 0 | NW flow |
| 28 Apr | Lubbock, TX | Cluster | 2 | 0 | Plains |
| 29 Apr | Goodland, KS | Squall line | 0 | 0 | Plains |
| 9 Nov | Louisville, KY | Squall line | 95 (LBE) | 2 | East |
| 2001 | | | | | |
| 16 Feb | Jackson, MS | Squall line | 60 (LBE) | 0 | Gulf |
| 12 Mar | Shreveport, LA | Squall line | 69 (LBE) | 1 | East |
| 24 Mar | Midland, TX | Cluster | 5 | 0 | NW flow |
| 29 Mar | Tallahassee, FL | Squall line | 28 | 0 | Gulf |
| 10 Apr | Topeka, KS | Squall-line/cell merger | 28 (LBE) | 26 | Plains |
| 14 Apr | Springfield, MO | Supercell | 4 | 0 | Plains |
| 15 Apr | Tulsa, OK | Squall line | 68 (LBE) | 0 | Plains |

echo start time (Fig. 4b) is seen in the early evening about 10 h after the maximum in the first-echo time. For all the bow echoes studies, bow-echo start time was at least 1.5 h after first-echo time, with a mean of 7 h (Fig. 5a). In a few events radar echoes were tracked for over 11 h between first-echo time and bow-echo start time. For example, radar echoes existed for 20 h prior to bow-echo start time in the 12 April 2000 event from the Lake Charles, Louisiana, WSR-88D. The maximum in the distribution of bow-echo end time (Fig. 4c) was

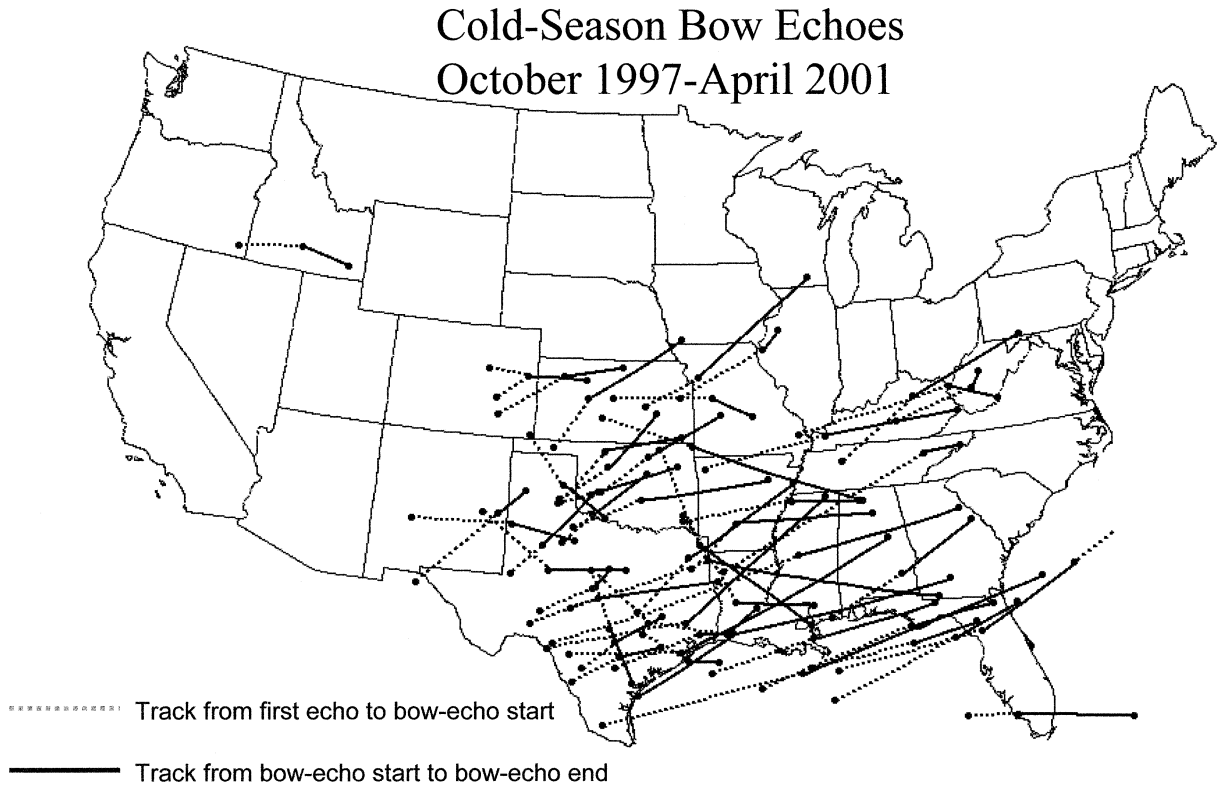


FIG. 2. Track map for 51 bow echoes that occurred during the cold seasons from Oct 1997 to Apr 2001. See section 2b for definitions of first-echo time, bow-echo start time, and bow-echo end time.

near midnight, just 2–3 h after the maximum in the distribution of bow-echo start time. Correspondingly, the distribution of bow-echo longevity has a strong peak between 2 and 3 h (Fig. 5b). A majority of the bow echoes observed had longevities of less than 8 h, although seven bow echoes lasted for more than 9 h. The longest-lasting bow echo, the 21 January 1998 event, which began near the Lake Charles, Louisiana, WSR-88D, lasted more than 16 h.

### *b. Supercells*

Supercells existed either in the formative or mature stages of 22 (43%) bow echoes. Ten (38%) of 26 squall-line bow echoes contained embedded supercells, the highest ratio of any development mode.

### *c. Environmental parameters*

Forty-six proximity soundings associated with 41 bow echoes were studied. The mean 0–2.5-km shear for bow echoes was 14 m $s^{-1}$, with 85% of the distribution lying between 5 and 20 m $s^{-1}$ (Fig. 6a). The mean 0–5-km shear was 23 m $s^{-1}$ with 69% of the distribution lying between 15 and 25 m $s^{-1}$ (Fig. 6b). Significant shear above 5 km was a characteristic of cold-season bow-echo environments; the mean 5–10-km shear was 19 m $s^{-1}$ (Fig. 6c). The mean CAPE for bow-echo environments was 1366 J $kg^{-1}$, with a normal distribution ranging from 0 to 3507 J $kg^{-1}$ (Fig. 6d). Sixty-five percent of cold-season bow echo environments had CAPE between 1000 and 2500 J $kg^{-1}$.

### *d. Bow-echo severity*

Altogether, the 51 bow echoes studies produced 899 reports of severe thunderstorm wind, an average of 17.6 reports per bow echo. Table 2 includes the number of severe thunderstorm wind reports associated with each bow echo. There was a pronounced break in the distri-

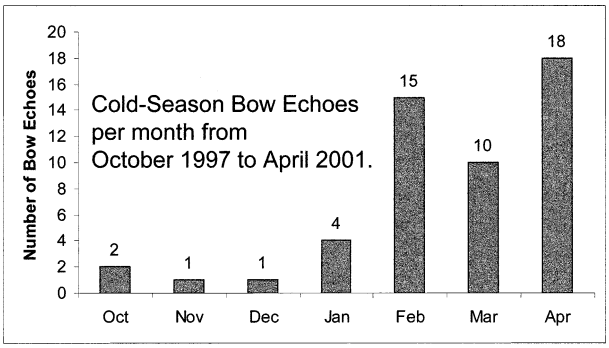


FIG. 3. Number of bow echoes per month during the cold seasons from Oct 1997 to Apr 2001.

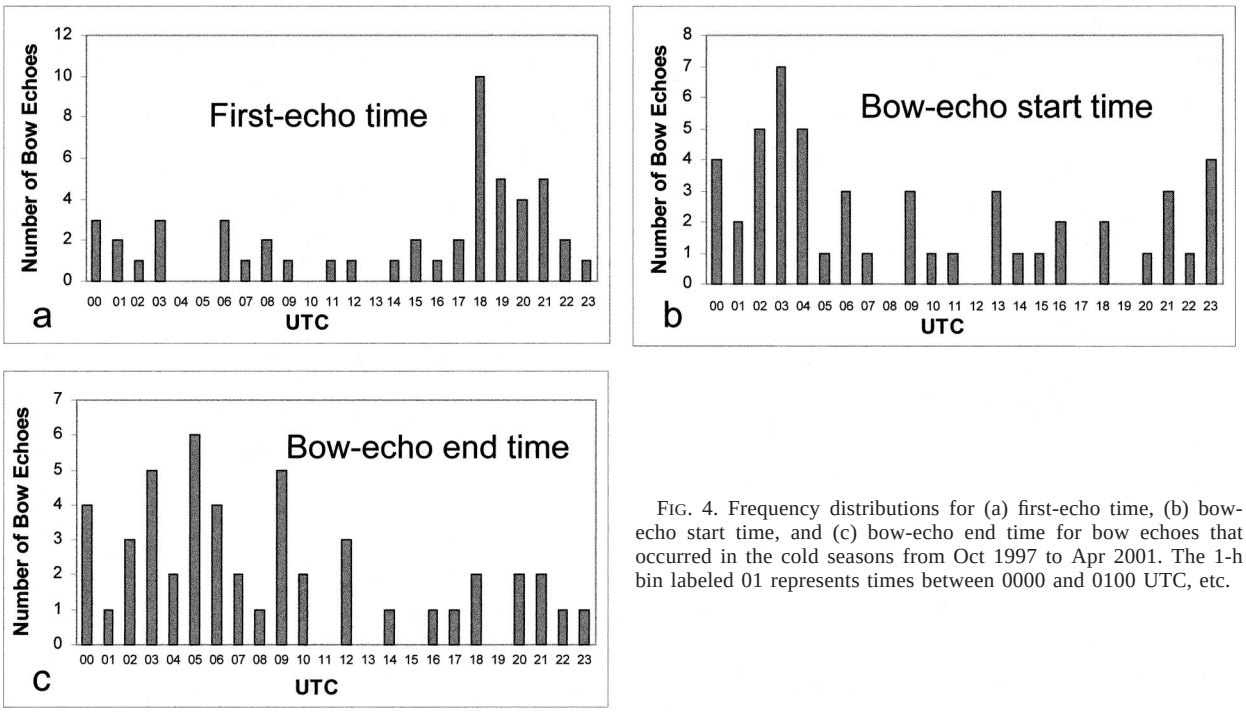


FIG. 4. Frequency distributions for (a) first-echo time, (b) bow-echo start time, and (c) bow-echo end time for bow echoes that occurred in the cold seasons from Oct 1997 to Apr 2001. The 1-h bin labeled 01 represents times between 0000 and 0100 UTC, etc.

bution of severe thunderstorm wind reports per bow echo. Most bow echoes (41) produced 20 or fewer severe thunderstorm wind reports. Two bow echoes produced exactly 28 reports, and one of those events met the definition of a derecho (Johns and Hirt 1987). The eight remaining bow echoes each produced 52 or more severe thunderstorm wind reports, and 6 of those events qualified as derechos. The union of derechos with bow echoes that produced 52 or more severe thunderstorm wind reports forms a set of nine very damaging bow echoes termed severe, long-lived bow echoes (LBEs). Cold-season LBEs occurred mainly in the southeastern states (Fig. 7).

From an idealized modeling study, Weisman (1993) hypothesized that LBEs represent a dynamically unique form of mesoconvective organization. This appears to be supported indirectly by the current findings. Eight of nine LBEs in this study produced at least 52 severe thunderstorm wind reports, which is at least 24 (86%) more than the number of reports that were associated with any non-LBE (bow echoes of lesser intensity and shorter duration than LBEs). Moreover, the nine LBEs produced a combined 55 tornadoes, including 26 tornadoes from a single LBE, whereas 40 of 42 (95%) non-LBEs did not produce any reported tornadoes (Table 2).

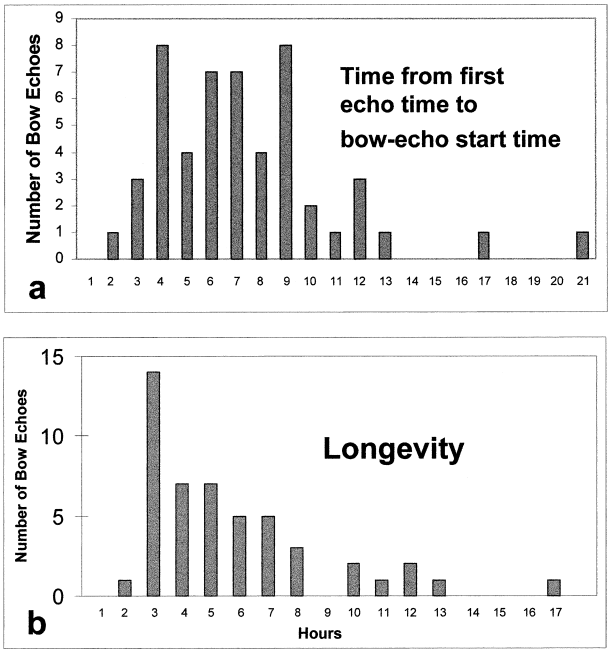


FIG. 5. Frequency distributions for (a) time from first-echo time to bow-echo start time and (b) bow-echo longevity. The 1-h bin labeled 1 represents duration times between 0 and 1 h. Note: the definition of bow echo in this study required longevity of at least 105 min.

### *e. Environments of LBEs*

#### 1) SYNOPTIC PATTERNS

Johns and Hirt (1987) showed that 90% of their dataset of warm-season derechos developed in westerly or northwesterly flow at 500 hPa. In contrast, 100% of the cold-season LBEs in this study developed when the 500-hPa wind was southwesterly, from between 205° and 265°, with a mean of 230°.

Johns and Hirt (1987) also showed that 40% of the warm-season derechos in their study developed in weak-

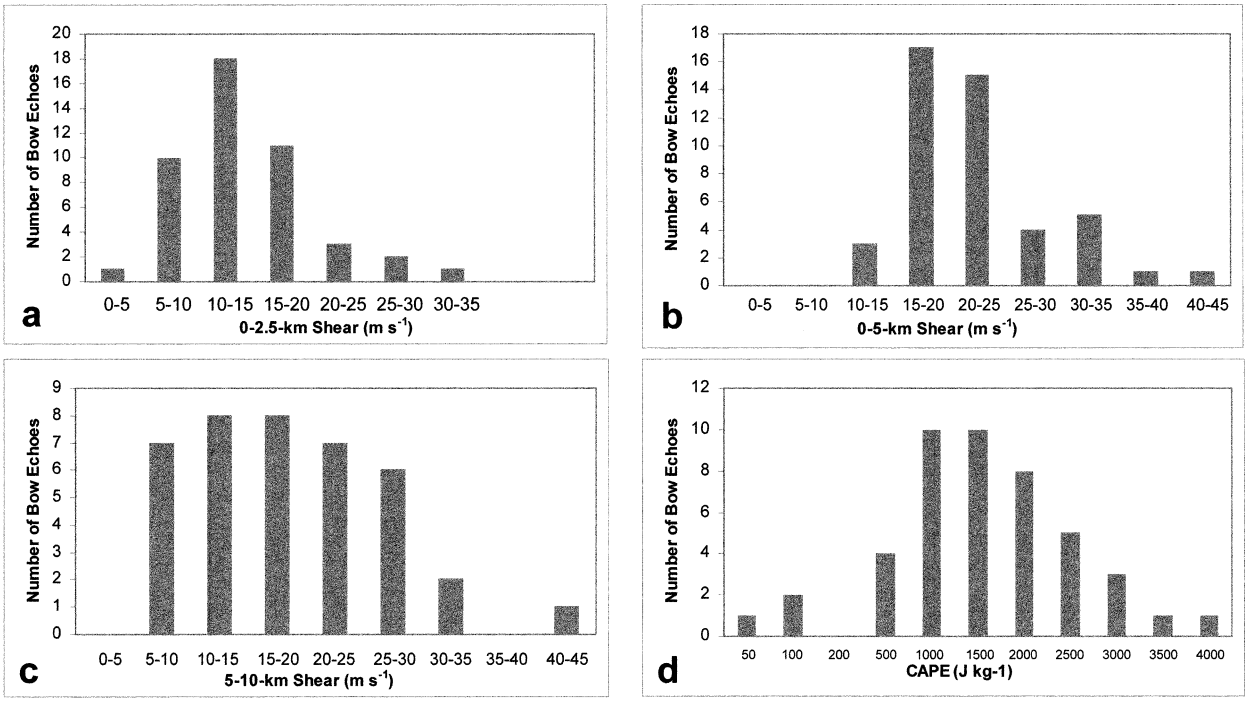


FIG. 6. Frequency distributions for (a) 0–2.5-km shear (m $s^{-1}$), (b) 0–5-km shear (m $s^{-1}$), (c) 5–10-km shear (m $s^{-1}$), and (d) CAPE (J $kg^{-1}$) for 46 bow-echo proximity soundings. The bin labeled 50 in (d) represents bow echoes whose proximity soundings indicated less than 50 J $kg^{-1}$ of CAPE. The bin labeled 100 represents bow echoes whose proximity soundings indicated greater than or equal to 50 J $kg^{-1}$ but less than 100 J $kg^{-1}$ of CAPE, etc.

ly forced synoptic patterns, ones in which low-level warm-air advection takes place on the cool side of a quasi-stationary surface boundary, often in a region characterized by extreme instability. During the cold season, stronger, more progressive synoptic-scale cyclones, reduced heating, and intrusions of cold, dry, continental air make extreme instability much less likely. All nine LBEs in this study developed in strongly forced synoptic patterns (e.g., Johns 1993; Evans and Doswell 2001) with low to moderate instability. One common thread, though, between warm-season derechos and cold-season LBEs was low-level warm-air advection. In 86% and 74%, respectively, of warm-season derechos they studied, Johns and Hirt (1987) found warm-air advection at 850 and 700 hPa at the initiation point. In this study, both 850 and 700-hPa warm-air advection were present at initiation of all nine LBEs.

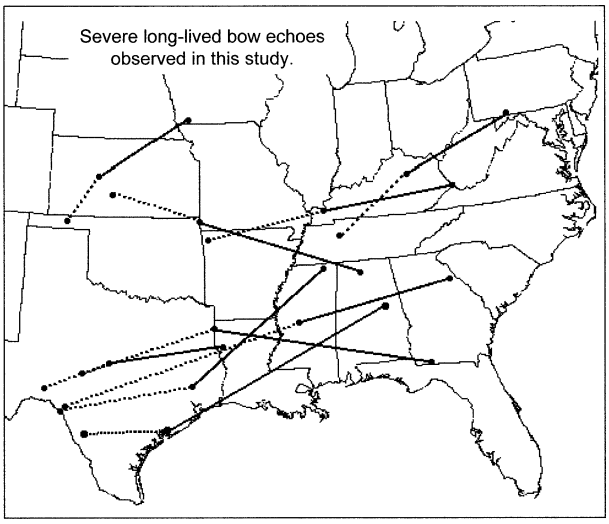


FIG. 7. Tracks of severe long-lived bow echoes observed during the cold seasons of Oct 1997–Apr 2001.

### 2) SHEAR AND CAPE

Idealized modeling studies of LBEs (e.g., Rotunno et al. 1988; Weisman et al. 1988; Weisman 1993) have emphasized the role of ambient vertical wind shear from the surface up to 5 km in sustaining the redevelopment of convection at the leading edge of long-lived squall lines and bow echoes. Weisman (1993) showed evidence that severe, long-lived bow echoes may be restricted to environments in which the component of vertical wind shear perpendicular to the bow echo is at least 20 m $s^{-1}$ over the lowest 5 km AGL. In this study, the component of 0–5-km shear perpendicular to the observed cold-season LBEs was generally at least 20 m $s^{-1}$, agreeing with the threshold suggested by Weisman (1993). Also, according to Weisman (1993), modeled LBEs are particularly favored when most of the shear is confined to

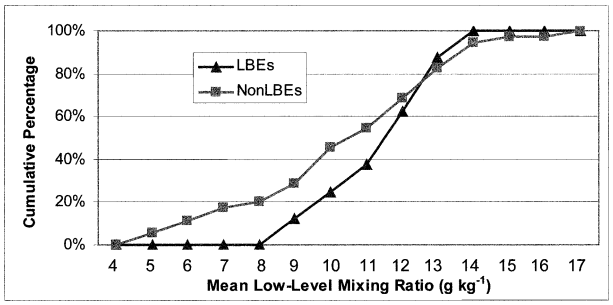


FIG. 8. Cumulative frequency distributions of mean low-level mixing ratio (g kg$^{-1}$) for LBEs and non-LBEs. The bin labeled 4 represents mean low-level mixing ratios less than 4 g kg$^{-1}$. The bin labeled 5 represents mean low-level mixing ratios greater than or equal to 4 g kg$^{-1}$ but less than 5 g kg$^{-1}$, etc.

the lowest 2.5 km AGL. In this study, however, the component of 0–2.5-km shear perpendicular to the bow echo was less than 20 m s$^{-1}$ for six of eight LBE proximity soundings, and was as low as 7.8 m s$^{-1}$ in the Fort Worth, Texas, derecho on 26 April 1999. Evans (1998) also found that many observed LBEs are associated with 0–2.5-km shears below 10 m s$^{-1}$. Coniglio and Stensrud (2001) have shown that shear above 5 km may also play an important role in maintaining some strong, long-lived squall lines (or bow echoes). In the current study, all LBE proximity soundings show 5–10-km shear that is comparable in magnitude to the observed low-level and midlevel shears, with the mean 5–10-km shear being 21 m s$^{-1}$.

Weisman (1993) also showed evidence that derechos (or LBEs) are restricted to environments that include CAPE of at least 2000 J kg$^{-1}$. Observational studies, however, have shown that large CAPE is most necessary for derechos that occur in weakly forced environments that are primarily confined to the warm season (e.g., Johns 1993; Evans and Doswell 2001). In this study, only one of eight cold-season LBE proximity soundings indicated CAPE above 2000 J kg$^{-1}$, and four of eight (50%) LBE proximity soundings indicated CAPE below 1000 J kg$^{-1}$. Evans and Doswell (2001) found 25% of their derechos to have CAPE less than 1000 J kg$^{-1}$. In this study, three proximity soundings associated with the 9 November 2000, Louisville, Kentucky, and 10 February 1998, Houston, Texas, LBEs showed CAPE ranging between 76 and 522 J kg$^{-1}$, yet these low CAPE

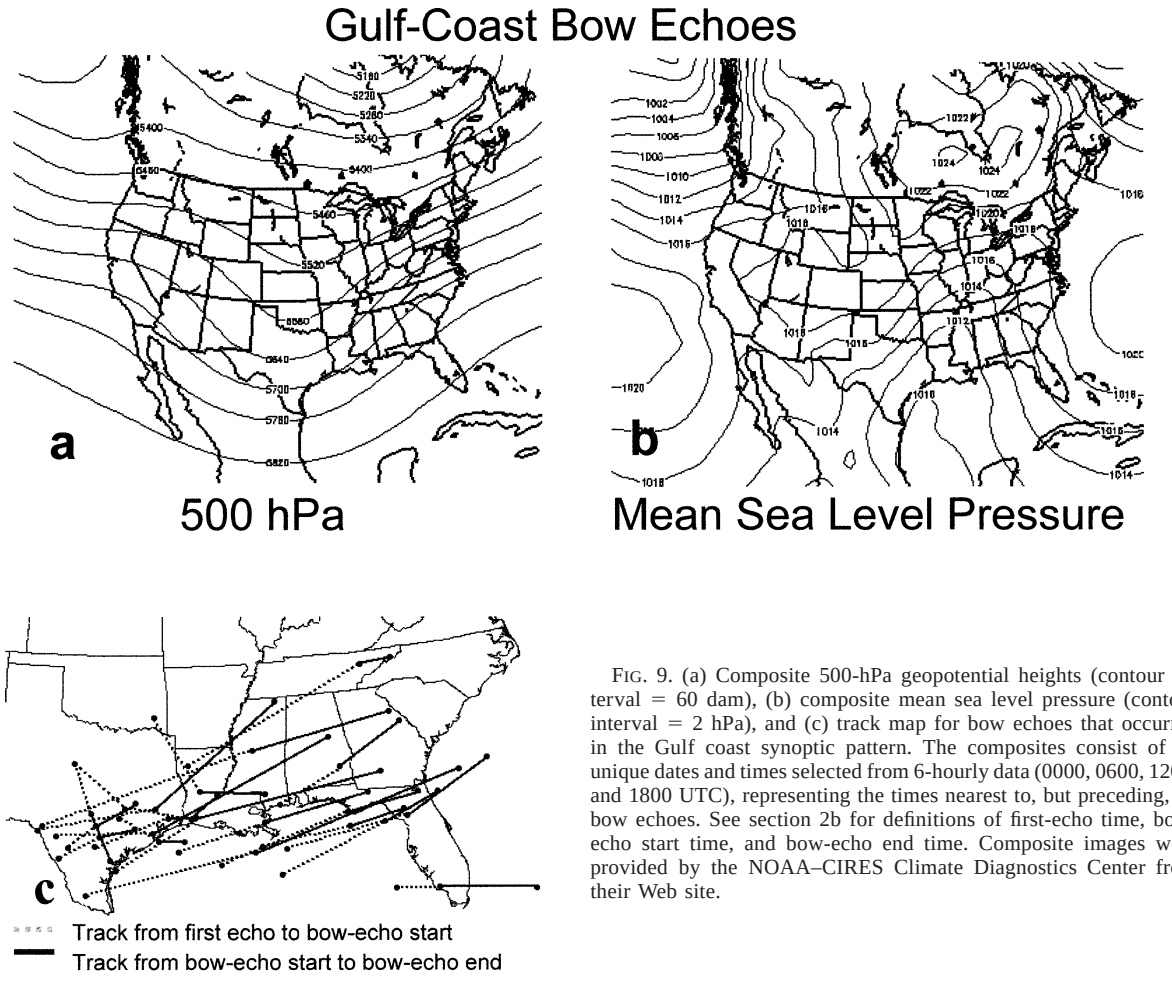


FIG. 9. (a) Composite 500-hPa geopotential heights (contour interval = 60 dam), (b) composite mean sea level pressure (contour interval = 2 hPa), and (c) track map for bow echoes that occurred in the Gulf coast synoptic pattern. The composites consist of 19 unique dates and times selected from 6-hourly data (0000, 0600, 1200, and 1800 UTC), representing the times nearest to, but preceding, 20 bow echoes. See section 2b for definitions of first-echo time, bow-echo start time, and bow-echo end time. Composite images were provided by the NOAA–CIRES Climate Diagnostics Center from their Web site.

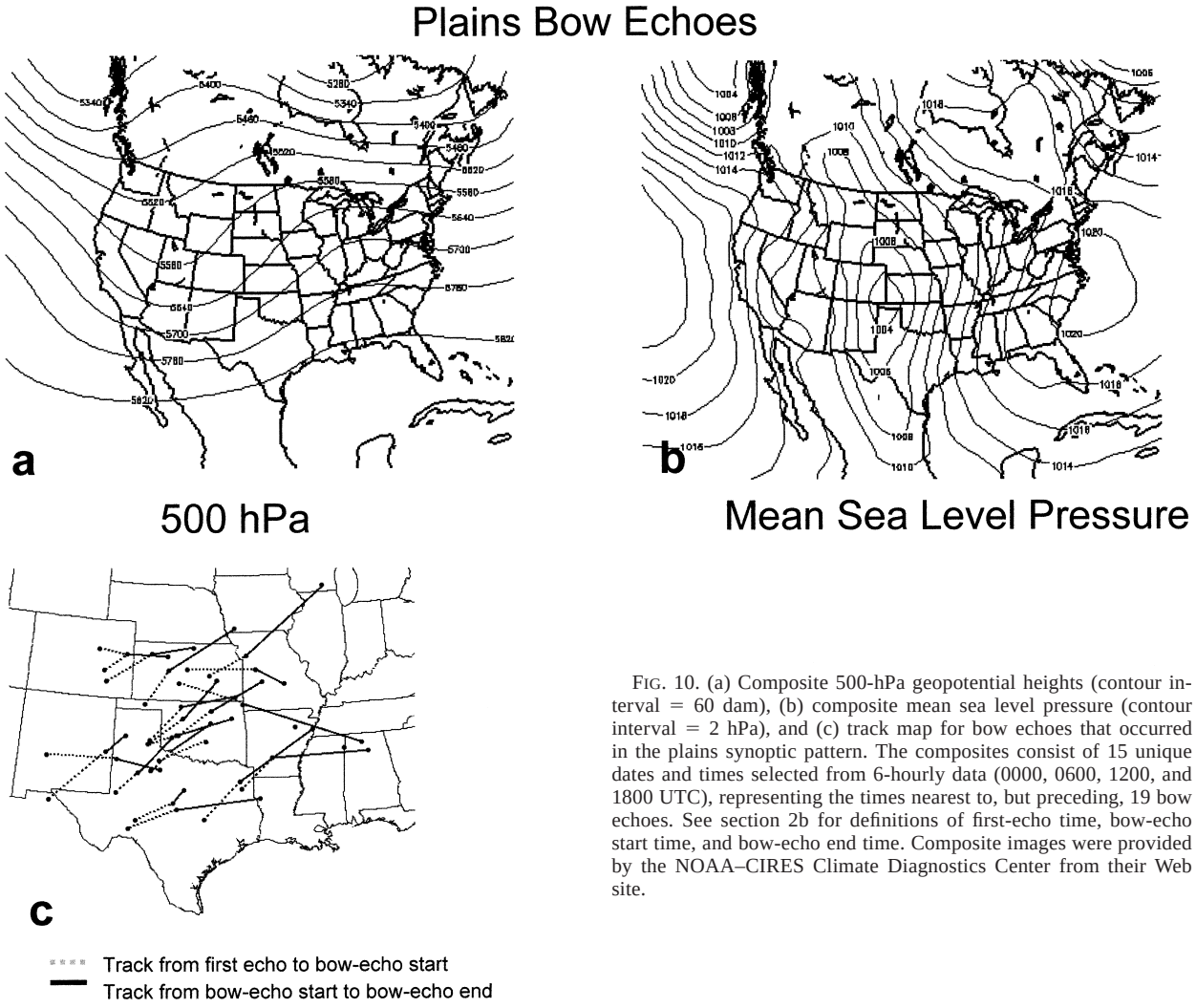


FIG. 10. (a) Composite 500-hPa geopotential heights (contour interval = 60 dam), (b) composite mean sea level pressure (contour interval = 2 hPa), and (c) track map for bow echoes that occurred in the plains synoptic pattern. The composites consist of 15 unique dates and times selected from 6-hourly data (0000, 0600, 1200, and 1800 UTC), representing the times nearest to, but preceding, 19 bow echoes. See section 2b for definitions of first-echo time, bow-echo start time, and bow-echo end time. Composite images were provided by the NOAA–CIRES Climate Diagnostics Center from their Web site.

events produced a combined 225 severe thunderstorm wind reports. Forecasters should be aware of the potential for severe long-lived bow echoes even when CAPE is very low (e.g., Evans and Doswell 2001).

Despite often low values of CAPE, abundant low-level moisture appears to be critical to the production of LBEs. The mean mixing ratio in the lowest 100 hPa AGL for LBE soundings was never less than 9 g kg$^{-1}$, with a mean of 11 g kg$^{-1}$ (Fig. 8). Abundant low-level moisture does not, however, make LBE environments distinct from environments in which other bow echoes formed. Thirty-three of the 43 (77%) non-LBE proximity soundings also indicated mean mixing ratios in the lowest 100-hPa AGL of at least 9 g kg$^{-1}$.

## 4. Synoptic patterns

Fifty cold-season bow echoes were associated with four synoptic patterns: Gulf coast, plains, east, and northwest flow. Three of the identified patterns correspond very well to bow echoes that formed in different geographical regions, hence the names Gulf coast, plains, and east. Composite maps of the time nearest, but preceding, bow-echo start (0000, 0600, 1200, or 1800 UTC), depicting the four synoptic patterns, were generated from the NOAA–Cooperative Institute for Research in Environmental Sciences (CIRES) Climate Diagnostics Center Web site (http://www.cdc.noaa.gov/) using the National Centers for Environmental Prediction–National Center for Atmospheric Research (NCEP–NCAR) reanalysis dataset (Kalnay et al. 1996).

### *a. Descriptions*

From late January to late April, 20 bow echoes occurred with a Gulf coast synoptic pattern that produced moderate instability and strong, deep shear over the Gulf of Mexico and southeastern states. Many Gulf coast events developed their first radar echoes in southern Texas and moved east-northeast (Fig. 9c). At 500 hPa, a broad long-wave trough was situated in the center of the United States (Fig. 9a). At the surface, a strong

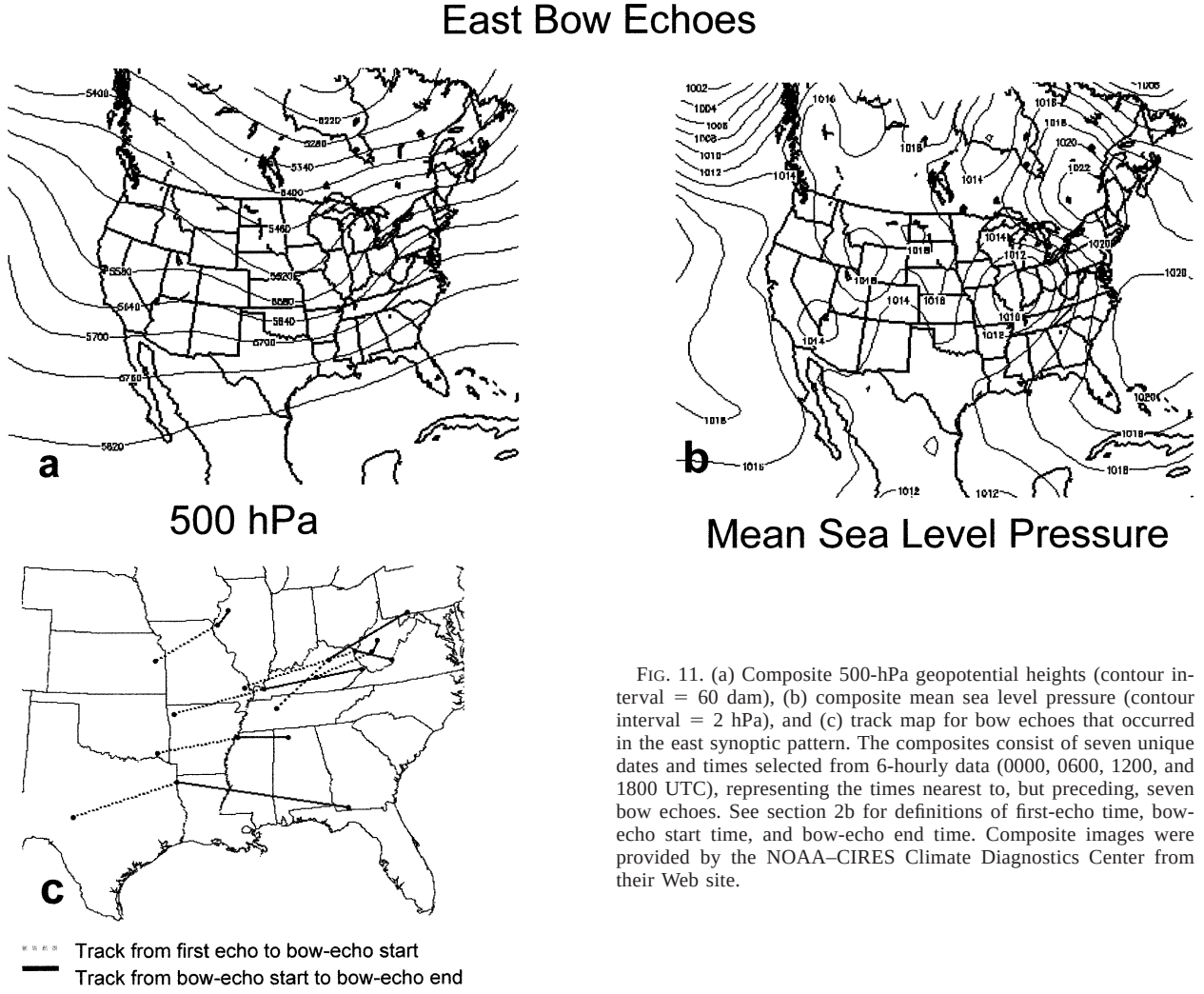


FIG. 11. (a) Composite 500-hPa geopotential heights (contour interval = 60 dam), (b) composite mean sea level pressure (contour interval = 2 hPa), and (c) track map for bow echoes that occurred in the east synoptic pattern. The composites consist of seven unique dates and times selected from 6-hourly data (0000, 0600, 1200, and 1800 UTC), representing the times nearest to, but preceding, seven bow echoes. See section 2b for definitions of first-echo time, bow-echo start time, and bow-echo end time. Composite images were provided by the NOAA–CIRES Climate Diagnostics Center from their Web site.

gradient existed between a closed low in the mean sea-level pressure (MSLP) field and a downstream high pressure center (Fig. 9b). Although shifted to other parts of the United States, both the 500-hPa long-wave trough and the strong MSLP gradient were common to the plains (Figs. 10a,b) and east (Figs. 11a,b) patterns as well.

Nineteen plains bow echoes occurred primarily from late February through April. Several plains bow echoes developed in Oklahoma after radar echoes were first detected near the Caprock region of the Texas Panhandle (Fig. 10c). A southerly low-level jet at 850 hPa over north-central Texas and southern Oklahoma, and a well-defined, southwesterly upper-level jet at 250 hPa, intersected at a large angle to produce strong deep-layer shear. The plains pattern is similar to the pattern favorable for severe thunderstorms and tornadoes first shown by Newton (1967). Johns (1993) also noted that the dynamic pattern for bow echoes ''has many characteristics of the 'classic' Great Plains tornado outbreak pattern.'' Two plains bow echoes were accompanied by tornado outbreaks.

The east pattern accounted for seven bow echoes and was similar to the plains pattern; the only major difference, aside from the geographical location of the features, is that the low-level jet was more parallel to the upper-level jet. Hence, the east pattern agrees well with the pattern Barnes and Newton (1986) showed to be favorable for the development of bow echoes. East bow echoes developed mainly in the lower Mississippi River valley (Fig. 11c).

Whereas 47 of 51 (92%) bow echoes occurred under southwesterly upper-level flow, only four bow echoes took place under northwest flow. Each of the four northwest flow bow echoes occurred in an amplified large-scale pattern with a broad 500-hPa ridge over the western United States and western Canada and a broad 500-hPa trough over the eastern United States and southeastern Canada (Fig. 12a). At the surface, high pressure was located over the Rockies and Great Plains (Fig.

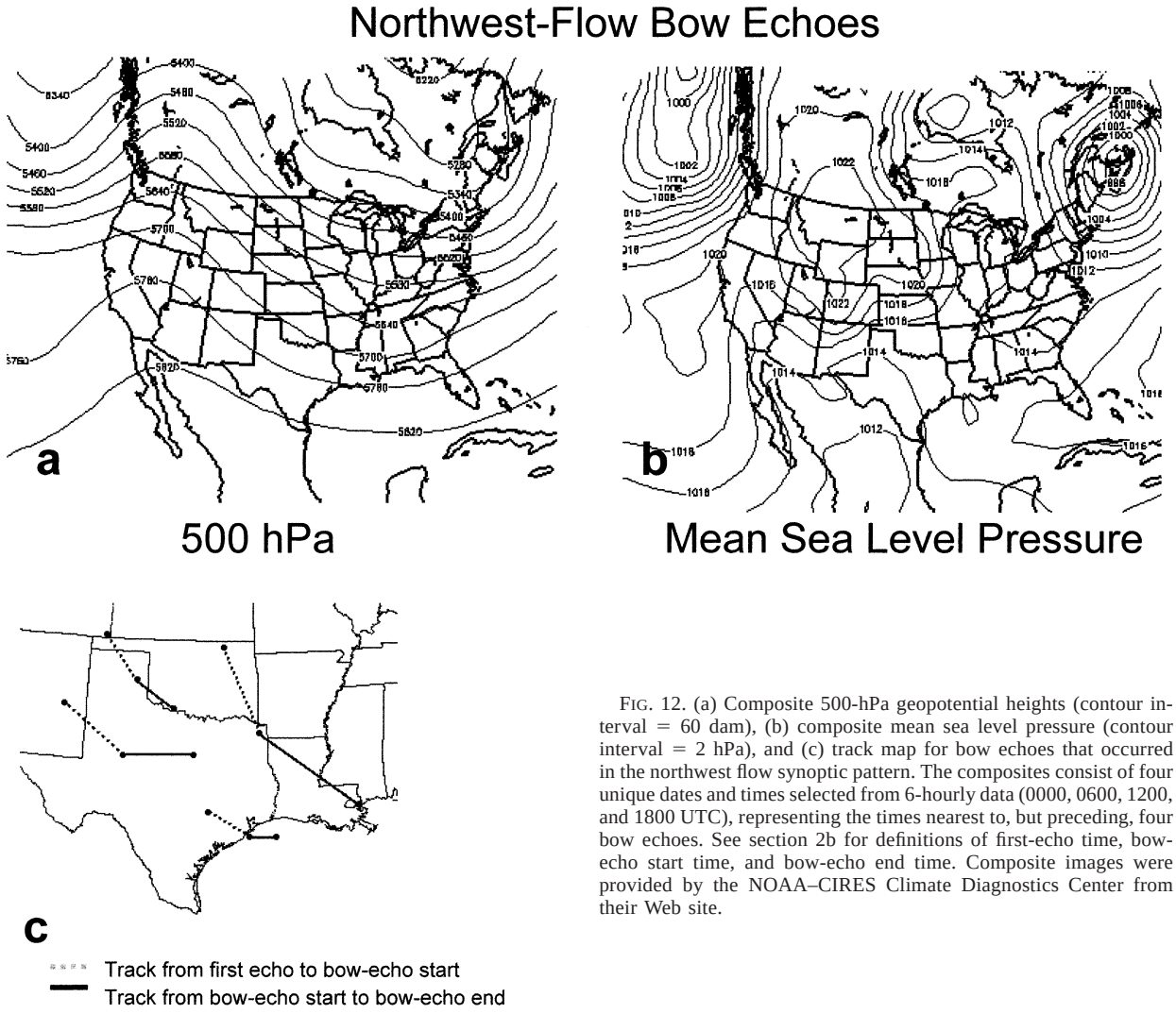


FIG. 12. (a) Composite 500-hPa geopotential heights (contour interval = 60 dam), (b) composite mean sea level pressure (contour interval = 2 hPa), and (c) track map for bow echoes that occurred in the northwest flow synoptic pattern. The composites consist of four unique dates and times selected from 6-hourly data (0000, 0600, 1200, and 1800 UTC), representing the times nearest to, but preceding, four bow echoes. See section 2b for definitions of first-echo time, bow-echo start time, and bow-echo end time. Composite images were provided by the NOAA–CIRES Climate Diagnostics Center from their Web site.

12b). Northwest flow bow echoes formed in Texas and Louisiana (Fig. 12c).

### *b. Comparisons*

The following discussion refers to information in Table 3. All mean shear values for the Gulf coast and plains patterns were very similar. The Gulf coast pattern had higher values of mean low-level mixing ratio (the highest of all patterns), while the plains pattern had higher mean CAPE (the highest of all patterns). The relatively high mean CAPE for the plains pattern was partially attributed to higher mean 850–500-mb lapse rates. The east pattern was seemingly deficient in CAPE, with a mean value, 705 J kg$^{-1}$, that was only about half as large as the mean CAPE in the Gulf coast and northwest flow patterns and a full 1000 J kg$^{-1}$ less than mean CAPE in the plains pattern. The east pattern exhibited

TABLE 3. Mean CAPE and shear values associated with four synoptic patterns in which bow echoes formed.

| Pattern (No. of events) | 0–2.5-km shear (m s$^{-1}$) | 0–5-km shear (m s$^{-1}$) | 5–10-km shear (m s$^{-1}$) | Mean low-level mixing ratio (g kg$^{-1}$) | 850–500-mb lapse rate (°C) | CAPE (J kg$^{-1}$) |
|---|---|---|---|---|---|---|
| Gulf coast (20) | 14.9 | 21.4 | 18.4 | 11.6 | 6.6 | 1295 |
| Plains (19) | 12.8 | 21.0 | 19.4 | 10.6 | 7.1 | 1711 |
| East (7) | 15.4 | 25.9 | 19.9 | 9.2 | 6.9 | 705 |
| Northwest (4) flow | 11.7 | 27.0 | 14.6 | 7.9 | 7.6 | 1287 |

the strongest mean shear values in all categories except when compared to the northwest flow pattern at 0–5 km. Interestingly, the east pattern also produced a relatively high percentage of LBEs. Three of 7 (43%) east pattern bow echoes were LBEs, compared to 3 of 20 (15%) and 3 of 19 (16%) for the Gulf coast and plains patterns, respectively. The northwest flow pattern had the strongest mean 0–5-km shear and nearly the second highest mean CAPE, yet no LBEs were observed in this pattern. The mean low-level mixing ratio, 7.9 g $kg^{-1}$, for northwest flow bow echoes was the lowest of any pattern, and this falls short of the 9 g $kg^{-1}$ that was found to be associated with all LBEs in this study. This result must be viewed with caution, as the sample size of northwest flow bow echoes is very small.

## 5. Conclusions

A search of radar mosaics and level-II WSR-88D data revealed 51 cold-season (October–April) bow echoes that occurred in the contiguous United States from 1997–98 to 2000–01. These are the key findings.

- Six development modes for bow echoes were observed, although most bow echoes evolved from squall lines (26), a group (or cluster) of cells (12), and squall-line–cell mergers (6).
- Supercells existed either in the formative or mature stages of 22 (43%) bow echoes, and in 10 (36%) of 26 bow echoes that developed from squall lines.
- Shear was usually moderate or strong. The mean 0–2.5-, 0–5-, and 5–10-km shear for bow echoes was 14, 23, and 19 m $s^{-1}$, respectively.
- The mean CAPE for bow-echo environments was 1366 J $kg^{-1}$, ranging from 0 to 3507 J $kg^{-1}$.
- There were nine severe, long-lived bow echoes (LBEs). LBEs developed in strongly forced, dynamic patterns with moderate instability. Environments of LBEs showed abundant low-level moisture (mean low-level mixing ratios of at least 9 g $kg^{-1}$).
- Cold-season bow echoes formed overwhelmingly (47 of 51) in southwesterly 500-mb flow, and four distinct synoptic patterns were identified. The synoptic patterns are associated with bow echoes that formed in the Gulf coast states, plains states, eastern states north of the Gulf coast states, and in northwest flow. A much higher percentage of bow echoes in the eastern states became LBEs compared to bow echoes in other patterns.

*Acknowledgments.* The authors would like to thank Joshua Palmer of North Carolina State University (formerly of NSSL) and the staff at NCDC whose help in providing level-II WSR-88D data was much appreciated. Don Burgess of NSSL and Dr. Howard Bluestein and Dr. Michael Richman of the University of Oklahoma lent helpful ideas and reviews when this work was first presented as a master's thesis. Robert Johns of the Storm Prediction Center also helped steer the research toward operationally important issues. Much of the text of this manuscript was improved through the constructive suggestions of two anonymous reviewers. Composite maps were provided by the NOAA–CIRES Climate Diagnostics Center, Boulder, Colorado, from their Web site (http://www.cdc.noaa.gov/). Funding was provided by NOAA/OAR/NSSL under NOAA–OU Cooperative Agreement NA17RJ1227.

## REFERENCES

Barnes, S. L., and C. W. Newton, 1986: Thunderstorms in the synoptic setting. *Thunderstorm Morphology and Dynamics*, 2d ed. E. Kessler, Ed., University of Oklahoma Press, 75–112.

Bentley, M. L., and T. L. Mote, 1998: A climatology of derecho-producing mesoscale convective systems in the central and eastern United States, 1986–95. Part I: Temporal and spatial distribution. *Bull. Amer. Meteor. Soc.,* **79,** 2527–2540.

——, and ——, 2000: A synoptic climatology of cool-season derecho events. *Phys. Geogr.,* **21,** 21–37.

——, and J. A. Sparks, 2003: A 15 yr climatology of derecho-producing mesoscale convective systems over the central and eastern United States. *Climate Res.,* **24,** 129–139.

Bluestein, H. B., and M. H. Jain, 1985: Formation of mesoscale lines of precipitation: Severe squall lines in Oklahoma during the spring. *J. Atmos. Sci.,* **42,** 1711–1732.

——, and S. S. Parker, 1993: Modes of isolated, severe convective storm formation along the dryline. *Mon. Wea. Rev.,* **121,** 1354–1372.

Brooks, H. E., C. A. Doswell III, and J. Cooper, 1994: On the environments of tornadic and nontornadic mesocyclones. *Wea. Forecasting,* **9,** 606–618.

Burke, P. C., 2002: A nationwide climatology of cold-season bow echoes. M.S. thesis, School of Meteorology, University of Oklahoma, 114 pp.

Coniglio, M. C., and D. J. Stensrud, 2001: Simulation of a progressive derecho using composite initial conditions. *Mon. Wea. Rev.,* **129,** 1593–1616.

Crum, T. D., and R. L. Alberty, 1993: The WSR-88D and the WSR-88D operational support facility. *Bull. Amer. Meteor. Soc.,* **74,** 1669–1688.

——, ——, and D. W. Burgess, 1993: Recording, archiving, and using WSR-88D data. *Bull. Amer. Meteor. Soc.,* **74,** 645–788.

Evans, J. S., 1998: An examination of observed shear profiles associated with long-lived bow echoes. Preprints, *19th Conf. on Severe Local Storms,* Minneapolis, MN, Amer. Meteor. Soc., 30–33.

——, and C. A. Doswell III, 2001: Examination of derecho environments using proximity soundings. *Wea. Forecasting,* **16,** 329–342.

Fujita, T. T., 1978: Manual of downburst prediction for Project NIMROD. Satellite and Mesometeorology Research Paper 156, Dept. of Geophysical Sciences, University of Chicago, 104 pp.

——, and E. Caracena, 1977: An analysis of three weather-related aircraft accidents. *Bull. Amer. Meteor. Soc.,* **58,** 1164–1181.

Glickman, T. S., Ed., 2000: *Glossary of Meteorology*. 2d ed. Amer. Meteor. Soc., 745 pp.

Hinrichs, G., 1888: Tornadoes and derechos. *Amer. Meteor. J.,* **5,** 306–317, 341–349.

Johns, R. H., 1993: Meteorological conditions associated with bow echo development in convective storms. *Wea. Forecasting,* **8,** 294–299.

——, and W. D. Hirt, 1987: Derechos: Widespread convectively induced windstorms. *Wea. Forecasting,* **2,** 32–49.

Kalnay, E., and Coauthors, 1996: The NCEP/NCAR 40-Year Reanalysis Project. *Bull. Amer. Meteor. Soc.,* **77,** 437–471.

Klimowski, B. A., R. Przybylinski, G. Schmocker, and M. R. Hjelm-

felt, 2000: Observations of the formation and early evolution of bow echoes. Preprints, *20th Conf. on Severe Local Storms,* Orlando, FL, Amer. Meteor. Soc., 44–47.

Lee, W. C., R. M. Wakimoto, and R. E. Carbone, 1992: The evolution and structure of a ''bow-echo–microburst'' event. Part II: The bow echo. *Mon. Wea. Rev.,* **120,** 2211–2225.

Miller, D. J., and R. H. Johns, 2000: A detailed look at extreme wind damage in derecho events. Preprints, *20th Conf. on Severe Local Storms,* Orlando, FL, Amer. Meteor. Soc., 52–55.

Newton, C. W., 1967: Severe convective storms. *Advances in Geophysics,* Vol. 12 Academic Press, 257–308.

Przybylinski, R. W., 1988: Radar signatures associated with the 10 March 1986 tornado outbreak over central Indiana. Preprints, *15th Conf. on Severe Local Storms,* Baltimore, MD, Amer. Meteor. Soc., 253–256.

——, 1995: The bow echo: Observations, numerical simulations, and severe weather detection methods. *Wea. Forecasting,* **10,** 203–218.

Rotunno, R., J. B. Klemp, and M. L. Weisman, 1988: A theory for strong, long-lived squall lines. *J. Atmos. Sci.,* **45,** 463–485.

Skamarock, W. C., M. L. Weisman, and J. B. Klemp, 1994: Three-dimensional evolution of simulated long-lived squall lines. *J. Atmos. Sci.,* **51,** 2563–2584.

Wakimoto, R. M., 1983: The West Bend, Wisconsin storm of 4 April 1981: A problem in operational meteorology. *J. Climate Appl. Meteor.,* **22,** 181–189.

——, 2001: Convectively driven high wind events. *Severe Convective Storms, Meteor. Monogr.,* No. 50, Amer. Meteor. Soc., 255–298.

Weisman, M. L., 1993: The genesis of severe, long-lived bow echoes. *J. Atmos. Sci.,* **50,** 645–670.

——, 2001: Bow echoes: A tribute to T. T. Fujita. *Bull. Amer. Meteor. Soc.,* **82,** 97–116.

——, J. B. Klemp, and R. Rotunno, 1988: Structure and evolution of numerically simulated squall lines. *J. Atmos. Sci.,* **45,** 1990–2013.

Williams, S., and S. Loehrer, 1996: Tactical data collection and management report for the GCIP Integrated Systems Test (GIST). IGPO Publication Series 20, 57 pp. [Available from Joint Office for Science Support (JOSS), University Corporation for Atmospheric Research (UCAR), P.O. Box 3000, Boulder, CO 80307.]